Ain Shams Engineering Journal (2012) 3, 49–59

Ain Shams University

Ain Shams Engineering Journal

www.elsevier.com/locate/asej
www.sciencedirect.com

MECHANICAL ENGINEERING

Thermal performance of the chilled water spirally coiled finned tube in cross flow for air conditioning applications

Abdalla Gomaa [a], Wael I.A. Aly [a,*], Ashraf Mimi Elsaid [a], Eldesuki I. Eid [b]

[a] *Department of Refrigeration and Air-Conditioning Technology, Faculty of Industrial Education, Helwan University, 11282 Cairo, Egypt*
[b] *Department of Mechanical Engineering, Faculty of Industrial Education, Suez Canal University, Suez, Egypt*

Received 29 May 2011; revised 5 October 2011; accepted 31 October 2011
Available online 13 January 2012

KEYWORDS

Heat transfer coefficient;
Spirally coiled tube;
Curvature ratio;
Pressure drop;
Heat exchanger

Abstract The thermal performance of spirally coiled finned tube in cross flow was investigated experimentally. The effects of curvature ratio, flow direction, fin pitch and flow rate of chilled water and air on thermal characteristics of spirally coiled finned tube have been studied. Six test sections with curvature ratios of 0.027, 0.03, 0.04, tube pitches of 18, 20, 30 mm, and fin pitches of 33, 22, 11 mm were used. The experiments were done using a pilot wind tunnel with air Reynolds number range 35,500–245,000. Innermost and outermost flow directions of chilled water with Reynolds number range 5700–25,300 have been investigated. The innermost flow direction has significant enhancement effect on the Nusselt number compared with outermost flow direction. The decrease of fin pitch enhances the Nusselt number on expense of pressure drop. Decreasing the curvature ratio increases air side Nusselt number on expense of pressure drop. A set of empirical expressions for predicting the friction factor and the Nusselt number for air flow across the spiral coils have been regressed based on the obtained data in the present experiments.

* Corresponding author. Tel.: +20 144614264.
E-mail address: aly_wael@yahoo.com (W.I.A. Aly).

Peer review under responsibility of Ain Shams University.
doi:10.1016/j.asej.2011.10.005

ELSEVIER Production and hosting by Elsevier

1. Introduction

Coiled tubes have higher heat transfer coefficient and smaller space requirement compared with straight tubes. Coiled tubes are the most widely used tubes in several heat transfer applications, for example, air conditioning and refrigeration systems, heat recovery processes, chemical reactors, and food and dairy processes. Helical and spiral coils are well known types of coiled tubes that have been used in a wide variety of applications. Moreover a number of papers are currently available on the helically coiled tube. It can be noted that the theoretical

Nomenclature

Symbol	Description
A	area (m^2)
C	specific heat ($kJ\,kg^{-1}\,K^{-1}$)
D	diameter (m)
De	Dean number
f	friction factor
h	heat transfer coefficient ($W\,m^{-2}\,K^{-1}$)
H	manometer head (m)
K	thermal conductivity ($W\,m^{-1}\,K^{-1}$)
L	length (m)
$\dot{m}$	mass flow rate ($kg\,s^{-1}$)
n	number of coil turn
N	number of fins
Nu	Nusselt number
p	pressure ($N\,m^{-2}$)
Δp	pressure drop ($N\,m^{-2}$)
Pr	Prandtl number
$\dot{Q}$	heat transfer rate (kW)
Q/P_P	heat transfer per unit pumping power
Re	Reynolds number
t	thickness of the fin (m)
T	temperature (°C)
U	overall heat transfer coefficient ($W\,m^{-2}\,K^{-1}$)
v	velocity ($m\,s^{-1}$)
w	width of fin (m)

Greek symbol

β	curvature ratio
ε	effectiveness
η	efficiency (%)
θ	manometer inclination angle (°)
λ	pitch (m)
μ	viscosity ($kg\,m^{-1}\,s^{-1}$)
ρ	density ($kg\,m^{-3}$)
$\varnothing$	diameter of spiral coil (m)

Subscripts

a	air
a	average
b	bulk
F	fin
h	hydraulic
i	inside
in	inlet
m	manometer
min	minimum
max	maximum
o	outside
p	pressure
s	surface
sc	spiral coil
t	total
tu	tube
w	water
$wall$	wall

and experimental investigations found in the literature focused on the study of the heat transfer and flow characteristics in a helical coiled tube.

Turbulent flow and convective heat transfer in a spirally coiled tube are complicated as comparing with the straight tube. This is due to the heat transfer and flow developments in the coiled tube that strongly depend on the behavior of secondary flow. The secondary flow in the coiled tube is caused by the centrifugal force.

Many different open literatures discuss the coiled tubes, due to the curvature of the tubes, as fluid flows through curved tubes, centrifugal force is generated. A secondary flow induced by the centrifugal force has significant ability to enhance the heat transfer rate. Dravid et al. [1] investigated numerically the effect of secondary flow on laminar flow heat transfer in helically coiled tubes. Patankar et al. [2] discussed the effect of the Dean number on friction factor and heat transfer in the helically coiled pipes. Yang et al. [3] presented a numerical model to study laminar convective heat transfer in a helicoidally pipe having a finite pitch. Rennie and Raghavan [4] simulated the heat transfer characteristics in a two-turn tube in-tube helical coil heat exchanger. The use of both active and passive techniques to enhance the heat transfer rate was reported by Cengiz et al. [5]. They studied the effect of rotation of helical pipes on the heat transfer rates and pressure drop for various air-flow rates. In their second paper [6], the heat transfer and pressure drop in a heat exchanger constructed by placing spring shaped wire with varying pitch were studied. The results indicated that the Nusselt number increased with decreasing pitch/wire diameter ratio. Kalb and Seader [7] carried out a theoretical study on the effect of the curvature ratio (radius of bend/inside radius of tube) on fully developed heat transfer in curved tubes with a uniform-wall-temperature. Naphon and Suwagrai [8] investigated the effect of curvature ratios on the heat transfer and flow developments in the horizontal spirally coiled tubes experimentally and numerically, which concluded that, due to the centrifugal force, the Nusselt number and pressure drop obtained from the spirally coiled tube are higher than those from the straight tube. The influences of centrifugal and buoyancy forces on the fully developed laminar flow in horizontal and vertical curved pipes under constant temperature gradient in the direction of the axis were studied by Yao and Berger [9]. Prusa and Yao [10] considered the combined effects of both buoyancy and centrifugal forces on the flow field and temperature distribution in flow for horizontal heated curved tubes. The numerical results indicated that the mass flow rate was drastically reduced because of the secondary flow.

Naphon and Wongwises [11] studied experimentally and numerically the heat transfer characteristics of a compact spiral coil heat exchanger, they found reasonable agreement between the results obtained from the experiment and those from the developed model. Due to the complexity of heat transfer and flow developments in spirally coiled tube, investigations on heat transfer in spiral-coil heat exchangers have received comparatively little attention in the literatures, as far as the authors know.

The main concern of the present work is to study the heat transfer and flow characteristics of spirally coiled tube in cross flow, which are used in air conditioning applications. Effects of curvature ratio, fin pitch, flow direction of chilled-water flow rate and pressure drop on heat transfer and flow characteristics are discussed and compared with those of flat bare and finned spiral coils in cross flow inside wind tunnel. Moreover, the present results are compared with available results in the literature.

2. Experimental apparatus and procedure

The experimental set up was composed of three cycles which are; open loop air passage, *R-22* Refrigeration cycle, and chilled water loop cycle. The experiments were conducted in a Plexiglas wind tunnel. The experimental test rig consists of a circular duct of 0.4 m diameter, 5 m length and 1.25 m height above ground equipped with a suction centrifugal fan as shown in Fig. 1. The fan motor has a power of 3.67 kW and it was linked with a variable speed frequency inverter having a capability to fine tuning the air velocity. The average air velocity in the test section is varied from 1.4 m/s to 9.6 m/s corresponding to Reynolds numbers from 35,500 to 245,000. Spirally coiled tubes that were located in the test section of the wind tunnel to construct a cross flow with air passage as illustrated in Fig. 2.

The close-loop of chilled water consists of a 0.1 m^3 storage insulated tank, and a refrigeration system which was controlled by adjusting thermostat to satisfy the supply water temperature to the heat exchanger. The chilled water was generated by the refrigeration system which was adjusted to the desired temperature using a temperature controller.

Six spiral-coils were designed and manufactured to perform this investigation. The total number of the test runs was 648 runs to get the results for the present study. The details of the geometry of the spiral coil test section are illustrated in Fig. 3. The geometric parameters of the spiral coils are provided in Table. 1. The chilled water was pumped from the storage tank to the spiral coil using 1 HP centrifugal pump and the flow rate was controlled by a ball valve and a flow meter with an accuracy of ±0.5% of full scale. The spiral coil surface temperatures were measured in 26 positions distributed along the perimeter of the spiral coil with K-type thermocouples as shown in Fig. 4. Before installation, all the thermocouples were calibrated at a number of temperatures against standard precision thermometer. Two groups of spirally coiled tube were used to satisfy the study, the first group is bare coils with different tube pitches, and the other one is finned coils with different fin pitches as shown in Fig. 5.

Before any data were recorded, the system was allowed to approach the steady state. Sufficient time was allowed to get the experimental measured parameters stabilized, which was observed to be about 40–50 min. Temperatures at each position and pressure drops were averaged over a time period.

3. Measuring techniques

The chilled water temperature was controlled and supplied to the heat exchanger with a temperature of 5 ± 0.5 °C. The inlet and the outlet temperatures of the water side were measured using two shelled pre-calibrated K-type thermocouples. A four grid points of the K-type thermocouple probes were fixed on the upstream and downstream of the test section, respectively

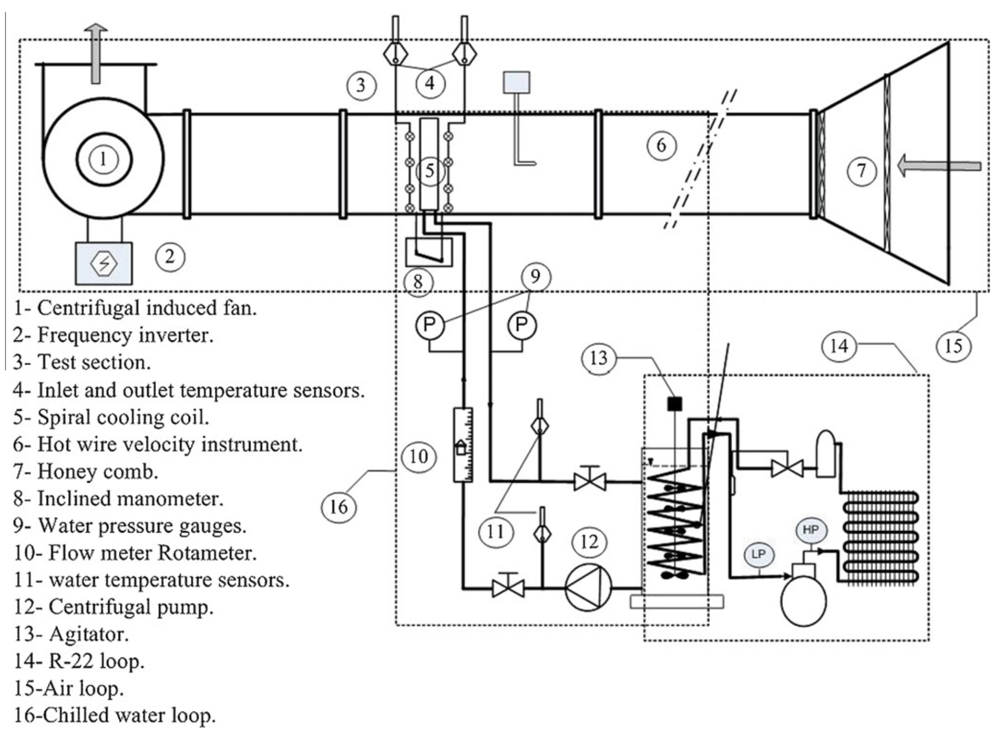

Figure 1 Schematic diagram of the experimental setup.

Figure 2 Photograph of the spiral coil inside the test section.

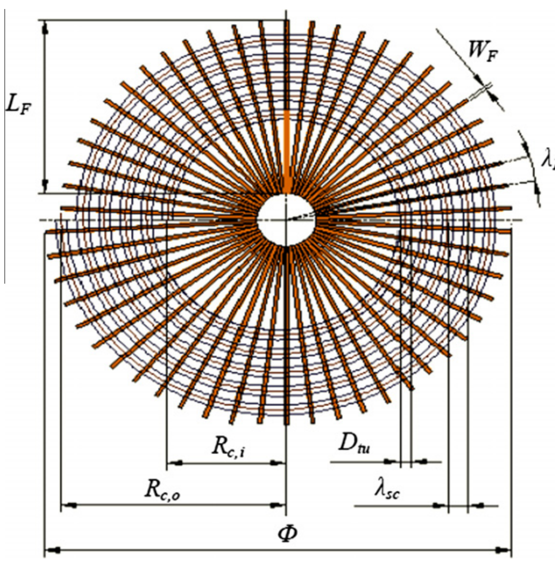

Figure 3 Schematic diagram of the spiral coil configuration.

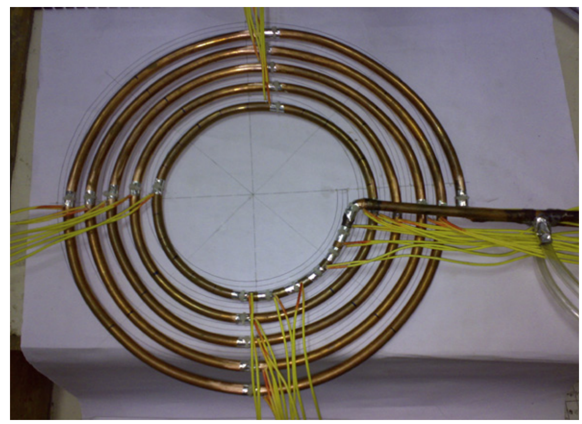

Figure 4 Photograph of thermocouples distribution along the spirally coiled tube surface.

to measure the air temperatures. All thermocouples were connected, via a switching box, to a digital thermometer. The water flow rate was measured using a flow meter with range of 1.8–18 l/min. The velocity profile of the air through the duct section was identified according to *ASHRAE* recommendations, [12] by hot wire anemometer with an accuracy of $\pm 0.01\%$ of full scale to get the average air velocity. The pressure drop of air a cross the heat exchanger (air side) was measured using an inclined manometer using a fluid known as Cyclo-hexane with chemical composition of CH_2 $(CH_2)_4$ CH_2, and its specific gravity is 0.7. The experimental program for the present study is given in Table 2.

4. Measurements uncertainties and accuracy

The experimental error analysis indicates the implication of error of the measured parameters on the uncertainty of the results. A detailed analysis of the various experimental uncertainties is carried out using the differential approximation method for error analysis [13]. The accuracy and uncertainty of the measurement are given in Table 3.

Table 1 Dimensions of the spirally coiled tubes.

Parameters	Coil-A	Coil-B	Coil-C	Coil-D	Coil-E	Coil-F
Outer diameter of tube, D_o (mm)	9.60	9.60	9.60	9.60	9.60	9.60
Inner diameter of tube, D_i (mm)	8.00	8.00	8.00	8.00	8.00	8.00
Length of spiral coils, L (mm)	4580	4200	4000	4580	4580	4580
Pitches of spiral coil, λ_{sc} (mm)	18	20	30	18	18	18
Curvature ratios (r_t/r_c), β	0.027	0.030	0.040	0.027	0.027	0.027
Number of coil turns, n_t	5	5	5	5	5	5
Number of fins, N_F	0	0	0	24	36	72
Dim. of fin $(L_F \times W_F \times t_F)$ (mm)	0	0	0	$170 \times 3 \times 1.3$		
Pitch of fins, λ_F (mm)	0	0	0	33	22	11

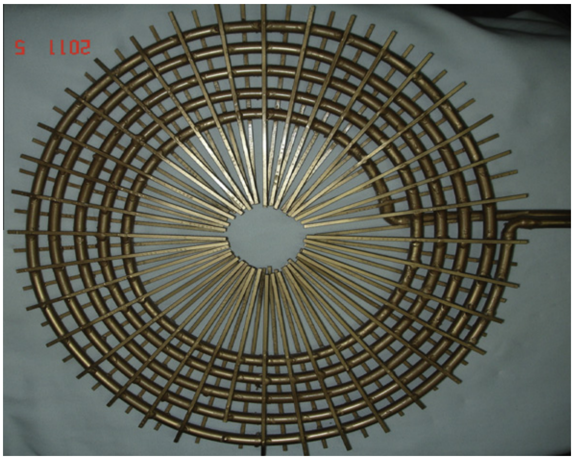

Figure 5 Photograph of the spiral finned cooling coil.

Table 2 Experimental conditions.

Variables/unit	Range	No. of readings
Inlet-chilled water temperature, °C	5 ± 0.5 °C	Constant
Inlet air velocity, m/s	$1.40 \leqslant v_a \leqslant 9.60$	12
Chilled water mass flow rate, kg/s	$0.05 \leqslant m_w \leqslant 0.14$	6

Table 3 Experimental uncertainty.

Instruments	Unit	Uncertainty (%)
Rotameter	kg/s	±1.43
Thermocouple K-type	°C	±0.18
Inclined manometer	mm	±1.61
Hot wire velocity	m/s	±1.55
Water gauge pressure	Bar	±4.67
Air heat transfer rate	kW	±5.83
Water heat transfer rate	kW	±4.69
Air Reynolds number	–	±4.59
Air friction factor	–	±5.23
Air Nusselt number	–	±8.61

5. Data reduction

The data reduction of the measured results is summarized in the following procedures.

Heat transferred to the air side, $\dot{Q}_a$ in the test section can be calculated as:

$$\dot{Q}_a = \dot{m}_a Cp_a (T_{a_i} - T_{a_o}) \tag{1}$$

Heat transferred to the cold water side, $\dot{Q}_w$ in the test section can be calculated as:

$$\dot{Q}_w = \dot{m}_w Cp_w (T_{w_o} - T_{w_i}) \tag{2}$$

The average heat transfer rate, $\dot{Q}_a$ used in the calculation was determined from the cold water side and air side as follows [14]:

$$\dot{Q}_a = 0.5(\dot{Q}_a + \dot{Q}_w) \tag{3}$$

The tube side (water side) heat transfer coefficient h_w can be calculated from the *Gnielinski* semi-empirical correlation Gnielinski [15]:

$$h_w = \left[\frac{K}{D_i}\right] \frac{(f_i/8)\mathrm{RePr}}{1 + 12.7\sqrt{f_i/8}(\mathrm{Pr}^{2/3} - 1)} \left(\frac{\mathrm{Pr}_b}{\mathrm{Pr}_{wall}}\right)^{0.14}$$
$$f_i = [0.3164/\mathrm{Re}^{0.25} + 0.03\beta^{0.5}]\left(\frac{\mu_{wall}}{\mu_b}\right)^{0.27} \tag{4}$$

The dimensionless group, Re_a and Nu_a can be determined from the following equations:

$$\mathrm{Re}_a = \frac{\rho D_h}{\mu}$$
$$\mathrm{Nu}_a = \frac{h_a D_h}{K} \tag{5}$$

The overall heat transfer coefficient, U_o can be determined as follows:

$$U_o = \frac{\dot{Q}_a}{A_t(LMTD)F} \tag{6}$$

An outside heat transfer coefficient (air side), h_a is usually obtained from the overall heat transfer coefficient by the following equation:

$$\frac{1}{U_o A_t} = \frac{1}{A_t h_a \eta_S} + \frac{\ln(D_o/D_i)}{2\pi K L_s} + \frac{1}{A_i h_w} \tag{7}$$

Surface efficiency, η_S is calculated as a function of fin efficiency by the following equation:

$$\eta_S = 1 - \frac{A_F}{A_t}(1 - \eta_F) \tag{8}$$

The fin efficiency, η_F is calculated by the following equation:

$$\eta_F = \frac{\tanh aL}{aL} \tag{9}$$

where a is a variable, which calculated by the following equation:

$$a = \sqrt{\frac{h_o P}{K_F A_C}} = \sqrt{\frac{2h_o}{K_F t_F}} \tag{10}$$

The friction factor for air across the spiral coil, f_a calculated from the following equation:

$$f_a = \frac{2\Delta p_a}{\rho_a V_a^2} \tag{11}$$

The heat transfer per unit pumping power for air side, $\frac{Q}{P_p}$ can be calculated by:

$$\frac{Q}{P_p} = \frac{Cp_a \Delta T_a}{[\Delta P_a/\rho_a]} \tag{12}$$

The effectiveness of the heat exchanger, ε can be calculated from the following equation:

$$\varepsilon = \frac{\dot{Q}_a}{\dot{Q}_{\max}} = \frac{\dot{Q}_a}{[(\dot{m}Cp)_{\min.}(T_{a_i} - T_{w_i})]} \tag{13}$$

6. Results and discussion

The air-side heat transfer, heat transfer per unit pumping power, and friction characteristics of all tested samples were determined from the experimental data. The spiral coil performance and heat transfer characteristics examined in this study at different curvature ratios of (0.027, 0.030 and 0.040) and different fin pitches of (11, 22 and 33 mm) corresponding to spirally coiled central angle of (10°, 20° and 30°), respectively.

The air Nusselt number of the spirally coiled tubes is plotted versus air Reynolds number for three different curvature ratios as shown in Fig. 6 for a range of $35{,}500 \leqslant \mathrm{Re}_a \leqslant 245{,}000$ at a constant chilled water mass flow rate of 0.083 kg/s. It can be seen from the figure that the air Nusselt number of the spirally coiled tubes increases with the increase of air Reynolds number for all cases. Moreover, decreasing the curvature ratio increases the air Nusselt number at the same air Reynolds number. For the same values of chilled water mass flow rate 0.083 kg/s, at constant average air velocity of v_a = 5.7 m/s (Re_a = 144,000), the air Nusselt number for the spirally coiled tube-A with curvature ratio of β = 0.027 is higher than that of coil-C with curvature ratio β = 0.040 by approximately 33.7%. This can be attributed to the effect of the coil pitch (λ_{sc}) of the spirally coiled tube, as decreasing the coil pitch means increasing of the spiral coil length and increasing of centrifugal force which enhances the heat transfer coefficient. This result is confirmed by Naphon and Suwagrai [8], they mentioned that, due to higher radius curvature, the centrifugal force also increases. Therefore at a given water mass flow rate, the average Nusselt number for lower curvature ratio are higher than those for higher ones across the range of water mass flow rate.

The air side friction factor of the spirally coiled tubes is plotted versus air Reynolds number as illustrated in Fig. 7 for a range of $35{,}500 \leqslant \mathrm{Re}_a \leqslant 245{,}000$ at a constant chilled water mass flow rate of 0.083 kg/s. From the figure it is noticed that the friction factor of the spirally coiled tubes decreases with the increase of air Reynolds number for all cases. Also,

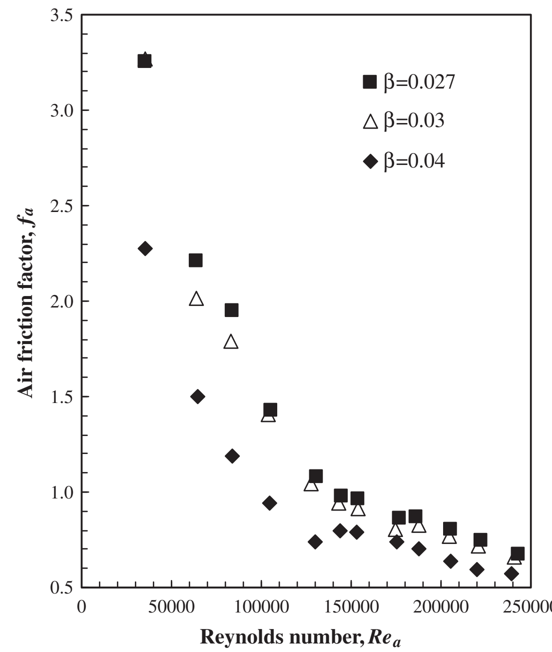

Figure 7 Air friction versus air Reynolds number for different curvature ratios at m_w = 0.083 kg/s.

it is seen that for the same air Reynolds number, decreasing the curvature ratio increase friction factor. For the same value of chilled water mass flow rate 0.083 kg/s, the friction factor of air side for the spirally coiled tube-A with curvature ratio of β = 0.027 is higher than that of coil-C with curvature ratio of β = 0.040 by approximately 18.2%. This can be attributed to the effect of the coil pitch (λ_{sc}) of the spirally coiled tube, as decreasing the coil pitch tends to increase the tube length and increases the surface area which affects the friction factor. This is in agreement with Wena and Ho [16] who reported similar conclusion.

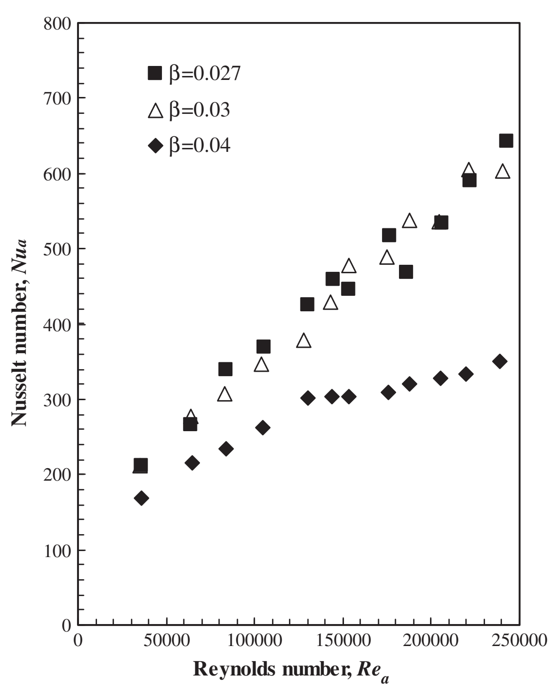

Figure 6 Air Nusselt number versus air Reynolds number for different curvature ratios at m_w = 0.083 kg/s.

Effectiveness is used to evaluate the performance of the spirally coiled heat exchanger. The effectiveness of the spirally coiled tubes against air Reynolds number are illustrated in Fig. 8 for a range of $35{,}500 \leqslant \mathrm{Re}_a \leqslant 245{,}000$ at a constant chilled water mass flow rate of 0.083 kg/s. The results indicated that the effectiveness decreases with the increase of air Reynolds number for all cases. Also, it is noted that the effectiveness increases with decreasing of curvature ratio. For the same values of average air velocity of v_a = 5.7 m/s (Re_a = 144,000), the effectiveness of the coil-A with curvature ratio of β = 0.027 is higher than that of coil-C with curvature ratio of β = 0.040 by approximately 33.6%.

The effect of water flow direction on air Nusselt number of the spirally coiled tubes is shown in Fig. 9 for a range of $35{,}500 \leqslant \mathrm{Re}_a \leqslant 245{,}000$ at a constant chilled water mass flow rate of 0.083 kg/s. The figure indicates that, the air Nusselt number for the spirally coiled tube-A with curvature ratio of β = 0.027 and innermost inlet flow direction is higher than the case of outermost inlet flow direction by approximately 49.7% for the same values of average air velocity of v_a = 5.7 m/s (Re_a = 144,000).

The relation between heat transfer per unit pumping power (Q/P_p) of the spirally coiled tubes and air Reynolds number is shown in Fig. 10 for a range of $35{,}500 \leqslant \mathrm{Re}_a \leqslant 245{,}000$ at a

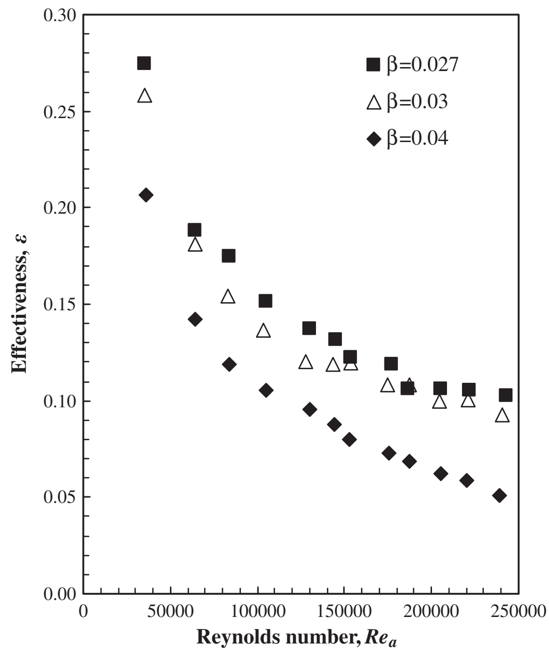

Figure 8 Effectiveness versus air Reynolds number for different curvature ratios at m_w = 0.083 kg/s.

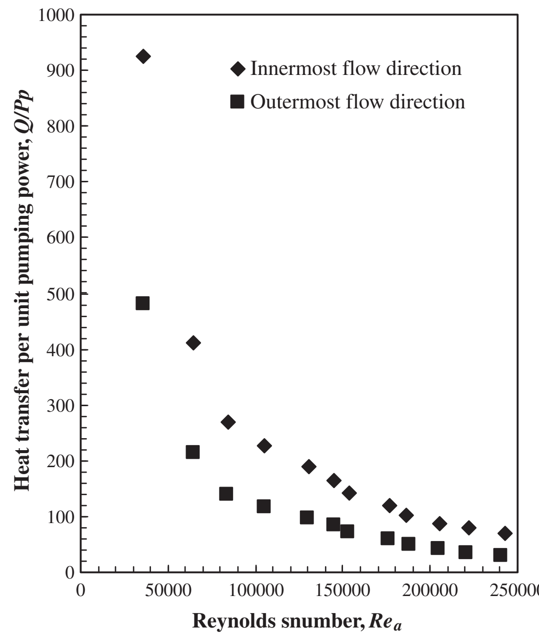

Figure 10 Heat transfer per unit pumping power versus air Reynolds number for different water flow direction at m_w = 0.083 kg/s.

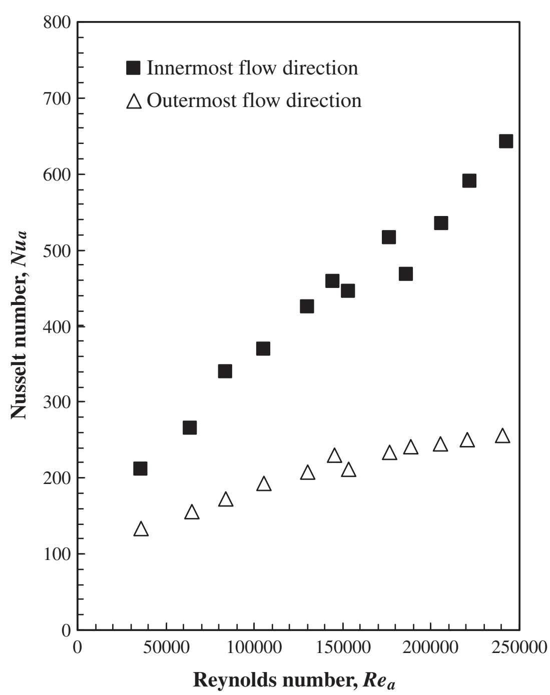

Figure 9 Air Nusselt number versus air Reynolds number for different water flow direction at m_w = 0.083 kg/s.

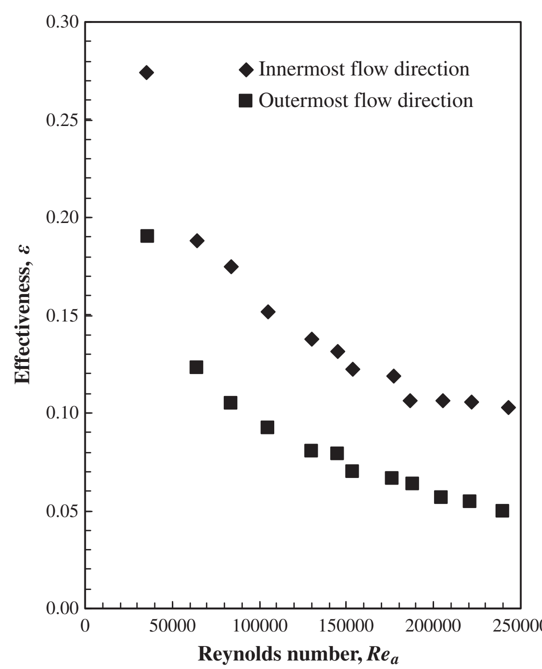

Figure 11 Effectiveness versus air Reynolds number for different water flow direction at m_w = 0.083 kg/s.

constant chilled water mass flow rate 0.083 kg/s. It is clear that the heat transfer per unit pumping power of the spirally coiled tubes decreases with the increase of air Reynolds number for all cases. At constant average air velocity of v_a = 5.7 m/s (Re_a = 143,990), the heat transfer per unit pumping power for the spirally coiled tube-A with curvature ratio of β = 0.027 and innermost inlet flow direction is higher than that of outermost inlet flow direction by approximately 55.8%.

Fig. 11 shows the relation between the effectiveness (ε) of the vertical cross flow spirally coiled tubes and air Reynolds number at a constant chilled water mass flow rate of 0.083 kg/s. It can be seen from this figure that the effectiveness of the spirally coiled tubes decreases with the increase of air Reynolds number for all cases. For the same values of average air velocity of v_a = 5.7 m/s (Re_a = 144,000), the effectiveness for the spirally coiled tube heat exchanger-A with curvature ratio of β = 0.027 and innermost inlet flow direction is higher than that of outermost inlet flow direction by approximately 40.2%.

The relation between air Nusselt number of the spirally coiled tubes and air Reynolds number for a range of $35{,}500 \leqslant Re_a \leqslant 245{,}000$ at a constant chilled water mass flow rate of 0.083 kg/s is shown in Fig. 12. It is understood that the air Nusselt number increases with the increase of air Reynolds number for all cases. Also, it is clear that decreasing the fin pitches increases the air Nusselt number for the same (Re_a). For the same values of average air velocity of v_a = 5.7 m/s (Re_a = 144,000), the air Nusselt number of the coil-F with fin pitches of λ_F = 11 mm, corresponding to the spiral coil central angle of 10° is higher than that of coil-A without fins λ_F = 0 by approximately 21.3%. This is due to the effect of the fin pitch (λ_F) of the spirally coiled tube, which increases the total exposed surface area of the coil.

The air heat transfer coefficient of the vertical cross flow spirally coiled tubes is plotted versus air pressure drop in Fig. 13 for a range of $4.1 \leqslant \Delta p_a \leqslant 38.1$, corresponding to air velocity range of $1.4 \leqslant v_a \leqslant 9.6$ at a constant chilled water mass flow rate of 0.083 kg/s. It is clear that the air heat transfer coefficient increases with the increase of air pressure drop for all cases. Moreover, decreasing the fin pitches (λ_F) increases the air heat transfer coefficient at the same air mass flow rate (m_a). For example, at a pressure drop of Δp_a = 20.9 Pa ($v_a = 5.7\ m/s$), the air heat transfer coefficient of the coil-F with fin pitches of λ_F = 11 mm is higher than that of coil-A without fins λ_F = 0 by approximately 21.2%. These results due to the fin pitch effect of the spirally coiled tube.

The effectiveness of the spirally coiled tubes is plotted versus air Reynolds number as illustrated in Fig. 14 for a range of $35{,}500 \leqslant Re_a \leqslant 245{,}000$ at a constant chilled water mass flow rate of 0.083 kg/s. It can be seen from this figure that the effectiveness decreases with the increase of air Reynolds number for all cases. This confirms the opinion of Wongwises and Naphon [17] who stated that the effectiveness decreases with the increase of air mass flow rate or Reynolds number. Also, it is noted that the effectiveness increases with increasing of fin pitches (λ_F). For the same values of air Reynolds number of Re_a = 144,000 (v_a = 5.7 m/s), the effectiveness of the coil-F with fin pitches of λ_F = 11 mm corresponding to the spiral coil central angle of 10° is higher than that of coil-A

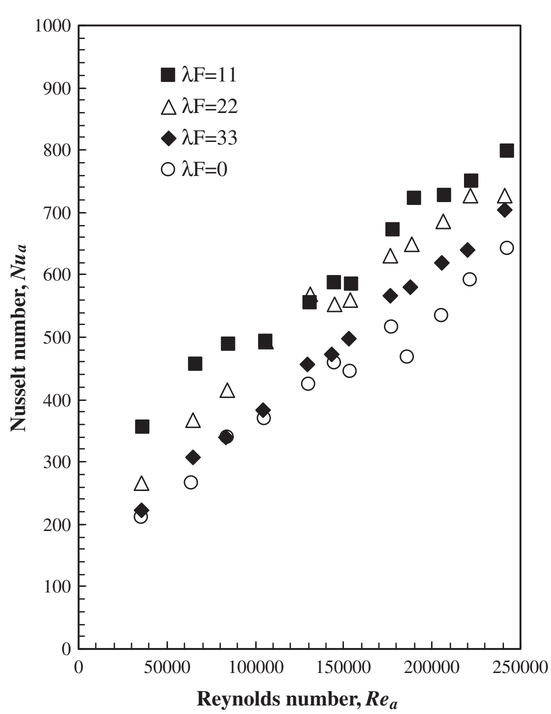

Figure 12 Air Nusselt number versus air Reynolds number for different fin pitches at m_w = 0.083 kg/s.

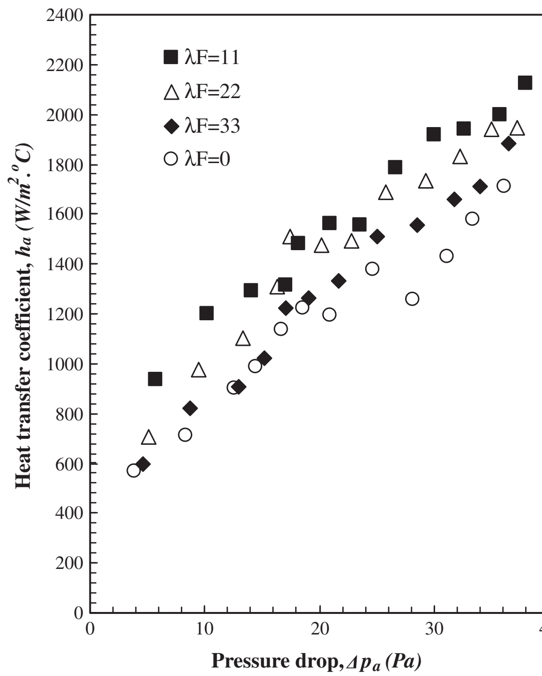

Figure 13 Heat transfer coefficient versus air pressure drop for different fin pitches at m_w = 0.083 kg/s.

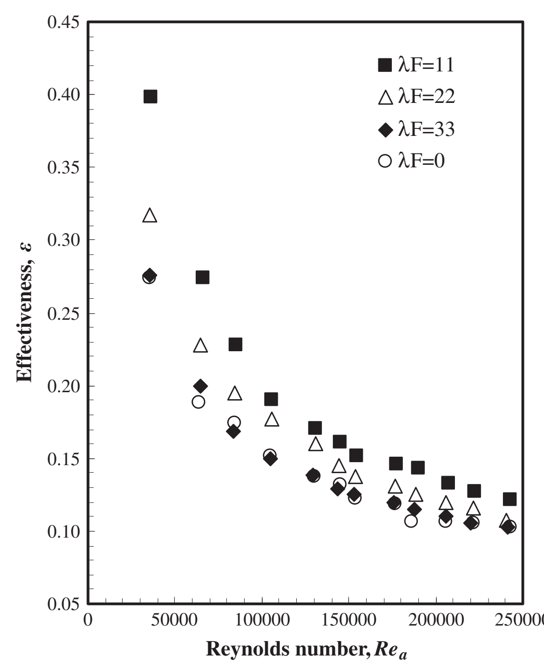

Figure 14 Effectiveness versus air Reynolds number for different fin pitches at m_w = 0.083 kg/s.

without fins $\lambda_F = 0$ by approximately 18.2%. This can be attributed to the effect of fin pitch of the spirally coiled tube as increasing the number of fins increases the heat transfer surface area. The air pressure drop of the vertical cross flow spirally coiled tubes is plotted versus average air velocity as illustrated in Fig. 15 for a range of $1.4 \leqslant v_a \leqslant 9.6$ at a constant chilled water mass flow rate of 0.083 kg/s. It can be seen from this figure that the air pressure drop increases with the increase of average air velocity for all cases. For the same values of average air velocity $v_a = 5.7$ m/s. As seen the air pressure drop increases with decreasing the fin pitch, for example, the air pressure drop of the coil-F with fin pitches of $\lambda_F = 11$ mm is higher than that of coil-A without fins $\lambda_F = 0$ by approximately 10.9%. This can be attributed by the disability of the fins to air flow through the spirally coiled tube. The air friction factor of the vertical cross flow spirally coiled tubes is plotted versus air Reynolds number as illustrated in Fig. 16 for a range of $35{,}500 \leqslant \mathrm{Re}_a \leqslant 245{,}000$ at a constant chilled water mass flow rate of 0.083 kg/s. It is noticed that the air friction factor decreases with the increase of air Reynolds number for all cases. For the same values of average air velocity $v_a = 2.54$ m/s, the friction factor of the coil-F with fin pitches of $\lambda_F = 11$ mm corresponding to the spiral coil central angle of 10° is higher than that of coil-A without fins $\lambda_F = 0$ by approximately 2.9%.

Fig. 17 shows the relation between the effectiveness of the spirally coiled tubes and air Reynolds number at a constant water Reynolds number (Re_w) of 25,300 for Srisawad and Wongwises [18] study and the present study. It can be seen from this figure that the effectiveness of the spirally coiled tubes decreases with the increase of air Reynolds number for all cases. Moreover, Fig. 18 shows the relation between the air Nusselt number of the spirally coiled tubes and air Reynolds number at a constant water Reynolds number of 25,300 for Srisawad and Wongwises [18] study and the present study. It can be seen from the figure that the air Nusselt number of the spirally coiled tubes increases with the increase of air Reynolds number for all cases.

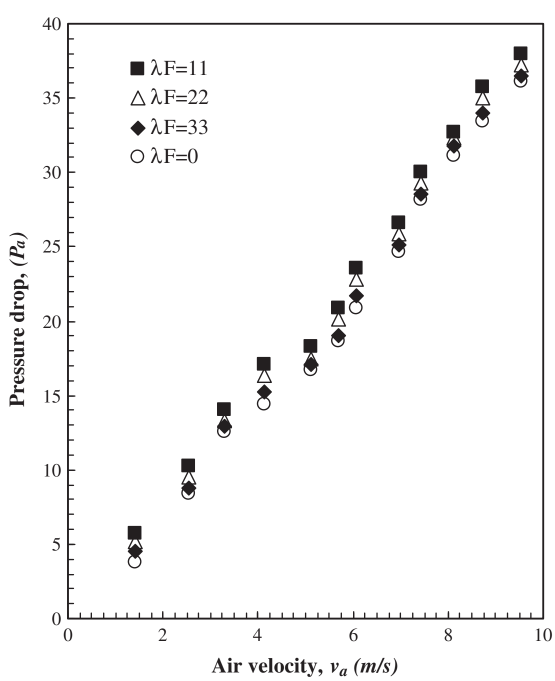

Figure 15 Air pressure drop versus air velocity for different fin pitches at $m_w = 0.083$ kg/s.

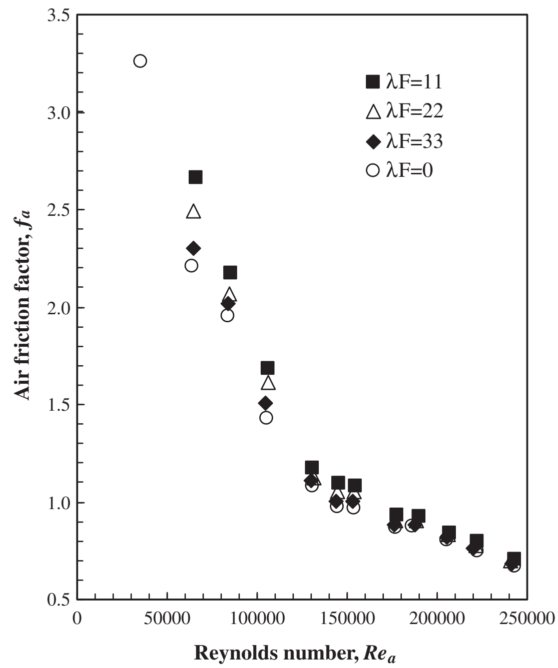

Figure 16 Air friction factor versus air Reynolds number for different fin pitches at $m_w = 0.083$ kg/s.

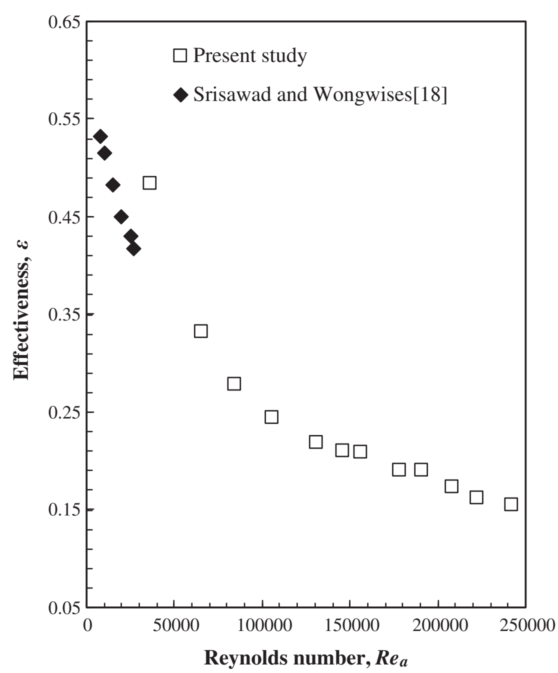

Figure 17 Effectiveness versus air Reynolds number for different studies.

Useful correlations to the practical applications for predicting the friction factor and the average Nusselt number for air flow across the spiral coils have been derived in terms of air Reynolds number Re_a, water Reynolds number Re_w, curvature ratio β, and number of fins N_f.

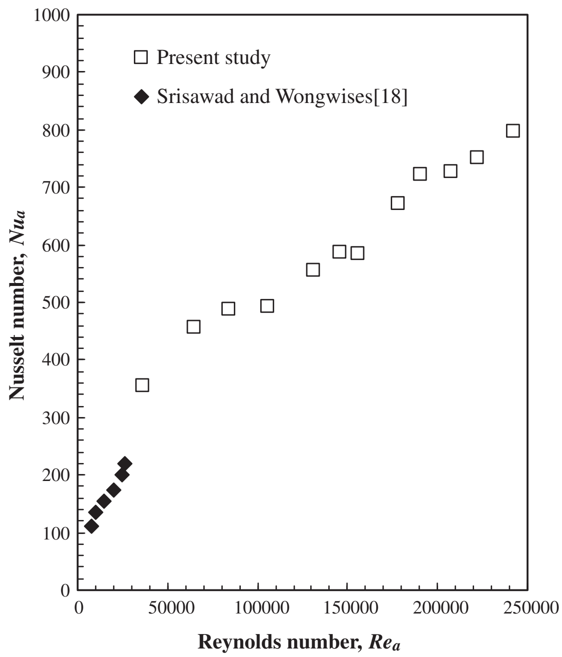

Figure 18 Air Nusselt number versus air Reynolds number for different studies.

6.1. Bare spirally coiled tube (innermost inlet flow direction and different tube pitches)

$$f_a = 6.41 \times 10^{-5} \mathrm{Re}_a^{-0.34} \mathrm{Re}_w^{0.47} \beta^{0.21} \tag{14}$$

$$\mathrm{Nu}_a = 3.28 \mathrm{Re}_a^{0.42} \mathrm{Re}_w^{0.55} \beta^{1.43} \tag{15}$$

Correlations (14) and (15) could predict the present data within a standard deviation of 15% and 14%, respectively, and they are applicable for the following conditions:

$$(35,500 \le \mathrm{Re}_a \le 245,000), (5700 \le \mathrm{Re}_w \le 25,300), \text{ and } (0.027 \le \beta \le 0.04)$$

6.2. Bare spirally coiled tube (outermost inlet flow direction and different tube pitches)

$$f_a = 6.67 \times 10^{-5} \mathrm{Re}_a^{-0.33} \mathrm{Re}_w^{0.47} \beta^{0.22} \tag{16}$$

$$\mathrm{Nu}_a = 0.008 \mathrm{Re}_a^{0.36} \mathrm{Re}_w^{0.4} \beta^{-0.615} \tag{17}$$

Correlations (16) and (17) could predict the present data within a standard deviation of 13% and 15%, respectively, and they are applicable for the following conditions:

$$(35,500 \le \mathrm{Re}_a \le 245,000), (5700 \le \mathrm{Re}_w \le 25,300), \text{ and } (0.027 \le \beta \le 0.04)$$

6.3. Finned spirally coiled tube (innermost inlet flow direction and different fin pitches (Number of fins))

$$f_a = 0.019 \mathrm{Re}_a^{-0.66} \mathrm{Re}_w^{1.92} N_F^{1.46\times10^{-4}} \tag{18}$$

$$\mathrm{Nu}_a = 0.01 \mathrm{Re}_a^{0.57} \mathrm{Re}_w^{0.38} N_F^{0.17} \tag{19}$$

Correlations (18) and (19) could predict the present data within a standard deviation of 17% and 9%, respectively, and they are applicable for the following conditions:

$$(35,500 \le \mathrm{Re}_a \le 245,000), (5700 \le \mathrm{Re}_w \le 25,300), \text{and} (24 \le N_F \le 72)$$

7. Conclusions

In the present investigation the effects of curvature ratio, air velocity, flow direction, water mass flow rate and fin pitch on the thermal performance of chilled-water spirally coiled tube in cross flow was examined experimentally. This type of heat exchanger consists of spirally coiled finned copper tube, with five turns. The effects of relevant experimental conditions are investigated in wind tunnel test rig. The main conclusions are summarized as follow:

- Decreasing the coil pitch increases the spiral coil length, increases the heat transfer surface area and air heat transfer coefficients. However the enhancement of heat transfer is on expense of pressure drop for the air side.
- The air heat transfer coefficient when using innermost flow direction of chilled water is higher than the outermost flow direction. Also, the heat transfer per unit pumping power is higher in case of using innermost flow direction of chilled water.
- Decreasing the fin pitch (or increasing the number of fins) enhances both of the air heat transfer coefficient and the effectiveness of spirally coiled tube, however increases the air pressure drop.
- The increasing of water mass flow rate participate a significant effect on the air-side heat transfer coefficient at the same air velocity.
- A set of empirical correlations for predicting the friction factor and the average Nusselt number for air flow across the spiral coils have been derived. These correlations are dependent on air Reynolds number Re_a, water Reynolds number Re_w, curvature ratio β, and number of fins N_f.

References

[1] Dravid AN, Smith KA, Merrill EW, Brain PLT. Effect of secondary fluid on laminar flow heat transfer in helically coiled tubes. AIChE J 1971;17:1114–22.

[2] Patankar SV, Pratap VS, Spalding DB. Prediction of laminar flow and heat transfer in helically coiled pipes. J Fluid Mech 1974;62:53–551.

[3] Yang G, Dong F, Ebadian MA. Laminar forced convection in a helicoidal pipe with finite pitch. Int J Heat Mass Trans 1995;38:853–62.

[4] Rennie TJ, Raghavan GSV. Laminar parallel flow in a tube-in-tube helical heat exchanger. In: AIC 2002 meeting CSAE/SCGR program. Saskatoon, Saskatchwan; 14–17 July, 2002.

[5] Cengiz Y, Yasar B, Dursun P. Heat transfer and pressure drops in rotating helical pipes. Appl Energy 1995;50:85–94.

[6] Cengiz Y, Yasar B, Dursun P. Heat transfer and pressure drops in a heat exchanger with a helical pipe containing inside springs. Energy Convers Manage 1997;38:619–24.

[7] Kalb CE, Seader JD. Fully developed viscous-flow heat transfer in curved circular tubes with uniform wall temperature. AIChE J 1974;20:340–6.

[8] Paisarn Naphon, Jamnean Suwagrai. Effect of curvature ratios on the heat transfer and flow developments in the horizontal spirally coiled tubes. Int J Heat Mass Trans 2007;50:444–51.

[9] Yao LS, Berger SA. Flow in heated curved pipes. J Fluid Mech 1978;88:339–54.

[10] Prusa J, Yao LS. Numerical solution for fully developed flow in heated curved tubes. J Fluid Mech 1982;123:503–22.

[11] Naphon Paisarn, Wongwises Somchai. A study of the heat transfer characteristics of a compact spiral coil heat exchanger under wet-surface conditions. Experim Thermal Fluid Sci 2005;29:511–21.

[12] ASHRAE handbook of fundamentals. SI edition, chapter 14, ASHRAE Inc., Atlanta, GA, USA; 2001.

[13] Holman JP. Experimental methods for engineers. 7th ed. New York, USA: McGraw-Hill Inc.; 2001.

[14] Nuntaphan Atipoang, Kiatsiriroat Tanongkiat. Thermal behavior of spiral fin tube bank under dehumidifying process: a case study of inline arrangement. Songklanakarin J Sci Technol 2004; 26(4).

[15] Volker Gnielinski. Heat transfer and pressure drop in helically coiled tubes. In: Proceedings of the 8th international heat transfer conference, vol. 6.Washington, DC: Taylor and Francis; 1986. p. 2847–54.

[16] Wena Mao-Yu, Ho Ching-Yen. Heat-transfer enhancement in fin-and-tube heat exchanger with improved fin design. Appl Therm Eng 2009;29:1050–7.

[17] Wongwises Somchai, Naphon Paisarn. Heat transfer characteristics and performance of a spirally coiled heat exchanger under sensible conditions. JSME Int J Ser B 2005;48(4).

[18] Srisawad Kwanchanok, Wongwises Somachai. Heat transfer characteristics of new coiled crimped spiral finned tube heat exchanger. Heat Mass Trans 2009;45:381–91.

Abdalla Gomaa is an Associate Professor and Head of Refrigeration and Air-conditioning Department, Faculty of Industrial Education, Helwan University at Cairo. He received his B.Sc. in Mechanical Power Engineering, Faculty of Engineering, Zagazig University, 1990, Egypt and his M.Sc. in Mechanical Power Engineering, Faculty of Engineering, Cairo University, Cairo, Egypt, 1996. In 2002 he received his Ph.D. in Thermofluids Engineering, Faculty of Engineering, Northumbria University at Newcastle, UK. In 2006 he spend nine menthes as Post-doctor research fellow, School of Built Environment, Northumbria University at Newcastle, United Kingdom. He has been actively working in the field of CFD in thermo-fluid engineering.

Wael I. A. Aly, is an Assistant Professor at the Refrigeration and Air-Conditioning Technology Department, Faculty of Industrial Education, Helwan University, Cairo, Egypt. He received his B.Sc. in Mechanical Power Engineering from Zagazig University (Egypt, 1994) and M.Sc. from Eindhoven University of Technology (The Netherlands, 1997). In 2007 he received his Ph.D. in Mechanical Power Engineering from Okayama University (Japan). Currently, Dr. Aly is a visiting assistant professor at Mechanical Engineering Department, Faculty of Engineering, King Khalid University (KSA). Dr. Aly current research fields are CFD, Thermofluids and Nanofluids.

Ashraf Mimi Elsaid Hassan, is a demonstrator at the Refrigeration and Air Conditioning Department of Technology, Faculty of Industrial Education, Helwan University, Egypt. He received his B.Sc. degree in Refrigeration and Air Conditioning Technology from Faculty of Industrial Education, Helwan University in 2000, and M.Sc. degree from Mechanical Department, Refrigeration and Air conditioning Division, Suez Canal University in 2011. In 2012 he will start studying Ph.D. in Suez Canal University. Currently, He has been actively working in the field of thermofluids.

Prof. Eldesouki Ibrahim Eid is now Professor of thermodynamics and heat transfer, Mechanical Department, Faculty of Industrial Education, Suez Canal University, Suez, EGYPT. Dr. Eid had B.Sc. in Mechanical Power Engineering, Faculty of Engineering, Menovia University, Cairo, Egypt, 1988. He had M.Sc. in Mechanical Power Engineering, Faculty of Engineering, Cairo University, Cairo, Egypt, 1995. He had Ph.D. in Mechanical Power Engineering, Faculty of Engineering, Ain Shams University, Cairo, Egypt, 2000. Dr. Eid worked as a lecture for about 5 years in Suez Canal University and about 5 years as associate professor. He was the chairman of the Mechanical Department for about 5 years and he was the Vice-Dean of Community service and Environmental Development Affairs for about one year. Now Prof. Eid is the vice-dean of the higher technological Institute, Science Valley Academy for the student's affairs. Prof. Eid is a reviewer in many international journals related to his specialist.